Optimal Field Sampling for

1. Exploration Target Zones and
2. Geochemical Characterization of Mine Tailings

P. Debba

CSIR, Logistics and Quantitative Methods, CSIR Built Environment

Outline

1. Introduction to Remote Sensing

2. Optimized sampling schemes case studies
    - Deriving optimal exploration target zones
    - Optimum sampling scheme for surface geochemical characterization of mine tailings

OVERVIEW OF HYPERSPECTRAL REMOTE SENSING

Hyperspectral sensors

- record the reflectance in many narrow contiguous bands
- various parts of the electromagnetic spectrum (visible - near infrared - short wave infrared)
- at each part of the electromagnetic spectrum results in an image

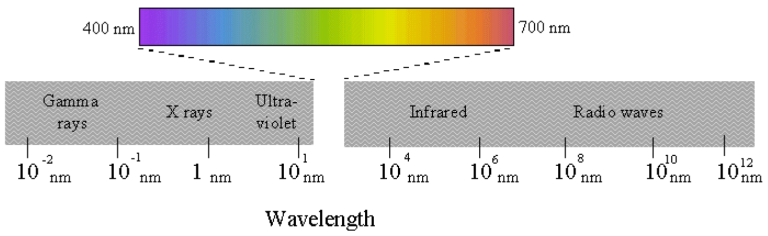

Figure: Spectral Range

OVERVIEW OF HYPERSPECTRAL REMOTE SENSING (cont. . .)

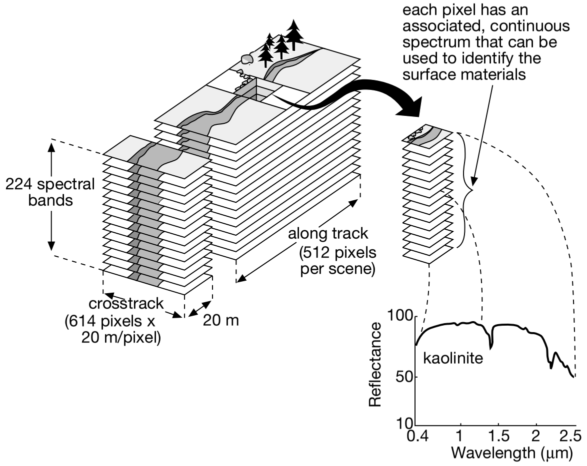

Figure: Hyperspectral cube

OVERVIEW OF HYPERSPECTRAL REMOTE SENSING (cont. . .)

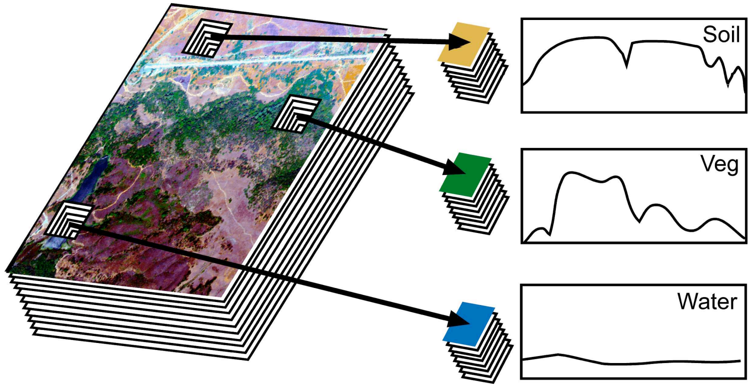

Figure: Pixels in hyperspectral image

OVERVIEW OF HYPERSPECTRAL REMOTE SENSING (cont. . .)

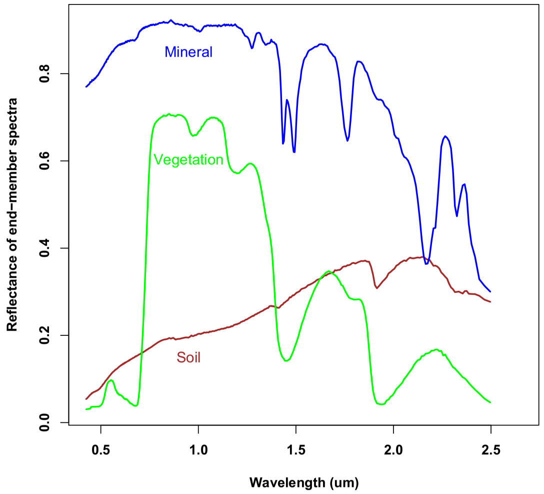

Figure: Example of 3 different spectral signatures

Outline

1. Introduction to Remote Sensing
2. Optimized sampling schemes case studies
    - Deriving optimal exploration target zones
    - Optimum sampling scheme for surface geochemical characterization of mine tailings

BACKGROUND AND OBJECTIVE OF STUDY

The location of known mineral occurrences (mines/prospects) are used for training in data-driven predictive mapping of prospective ground. Particular methods for obtaining a mineral prospective map are

- the weights-of-evidence (WofE) method
- logistic regression
- canonical favorability analysis
- neural networks
- evidential belief functions

BACKGROUND AND OBJECTIVE OF STUDY (cont. . .)

Mineral prospectivity maps are then usually used to guide further mineral exploration. A logical question regarding efficacy of mineral prospectivity maps is: “Where should targets of exploration for undiscovered mineral occurrences be focussed?”

The objective of this study is to demonstrate a methodology that we have developed in order to provide a plausible answer to the above question in a district-scale case study.

STUDY SITE

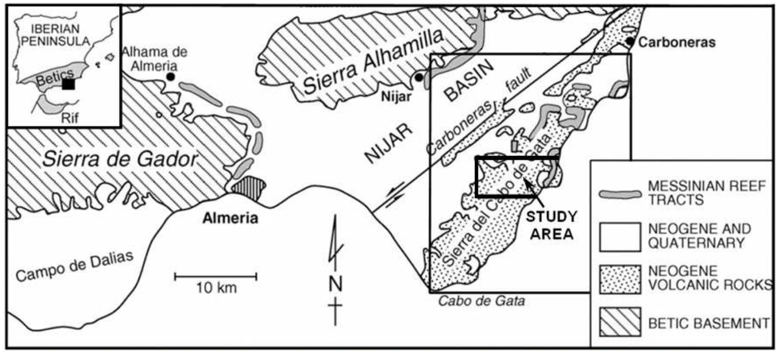

Figure: A generalized geological map of the Rodalquilar area mineral district.

DATA USED

- Two sets of locations of mineral deposit occurrences, from different sources, were used in WofE modeling.
- Set 1: 14 epithermal deposits and set 2: 36 epithermal deposits.
- Set 2: Training set for WofE and designing optimal exploration target zones.
- Set 1: Validation of WofE and optimal exploration target zones.
- HyMap: 126 bands – 0.4–2.5 μm
- Geology: 30 bands – 1.95–2.48 μm
- Distinctive absorption features at wavelengths near 2.2 μm

DATA USED (cont. . .): CREATION OF BAND RATIO AS EVIDENCES

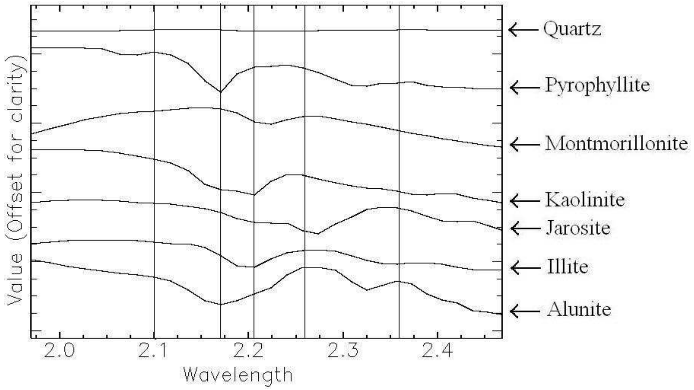

Figure: Plot of seven endmembers from USGS spectral library in the spectral range 1.95–2.48 μm. Vertical lines indicate the band centers used to obtain band ratio images (see text for further information).

DATA USED (cont. . .): CREATION OF BAND RATIO AS EVIDENCES

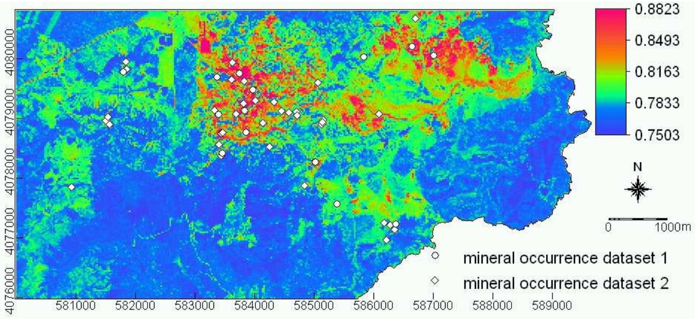

Figure: Band Ratio 1: arctan transformation on bands 103/107 (2.100/2.171 μm).

DATA USED (cont. . .): CREATION OF BAND RATIO AS EVIDENCES

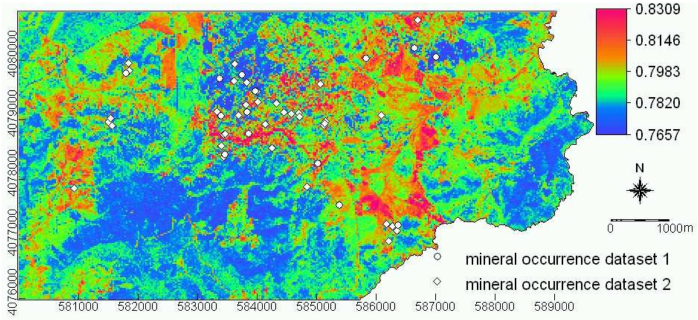

Figure: Band Ratio 2: arctan transformation on bands 107/109 (2.171/2.205 μm).

DATA USED (cont. . .): CREATION OF BAND RATIO AS EVIDENCES

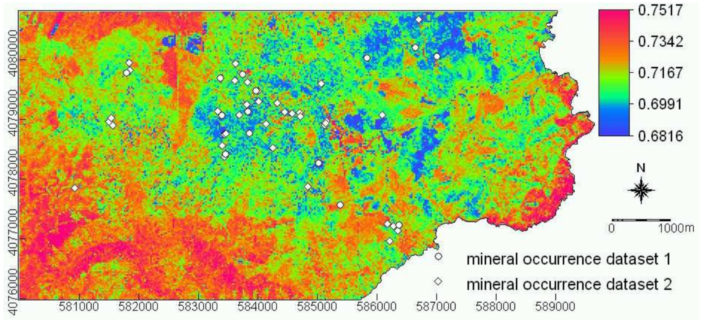

Figure: Band Ratio 3: arctan transformation on bands 118/112 (2.357/2.258 μm).

DATA USED (cont. . .): CREATION OF STRUCTURAL EVIDENCE

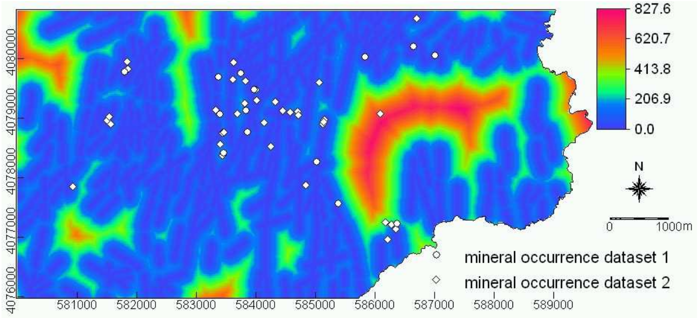

Figure: Distance to fault and fracture. Increasing pixel brightness in this image indicates increasing distance from a fault or fracture.

METHODS

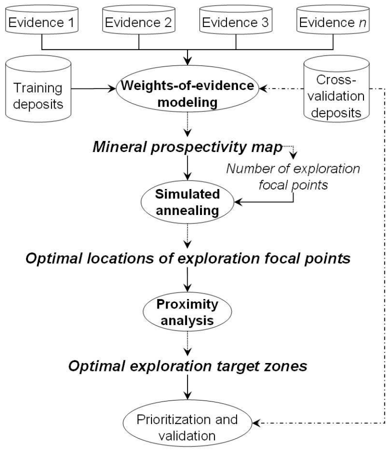

Figure: Flow diagram describing the process.

METHODS (cont. . .): ESTIMATION OF THE NUMBER OF EXPLORATION FOCAL POINTS

To estimate the number of exploration focal points, we used the binomial distribution – mineral deposit occurrence is a binary variable, being either present or absent.
Thus, estimation of n exploration focal points so as to yield (or discover) at least r mineral deposit occurrences, with a probability of success p, at a 95% confidence, requires a solution for the following equation:

$$\sum_{i=r}^{n} \binom{n}{i} p^i (1-p)^{n-i} = 0.95\,. \qquad (1)$$

METHODS (cont. . .): FITNESS FUNCTION

$$\begin{aligned}\phi_{\mathrm{WMSD+V}}(\mathbf{S}^n) &= \frac{\lambda}{N(A)} \sum_{\vec{\mathbf{x}} \in A} P(\vec{\mathbf{x}})\,\|\vec{\mathbf{x}} - Q_{\mathbf{S}^n}(\vec{\mathbf{x}})\| \\ &\quad + (1-\lambda)s^2(O_{\mathbf{S}^n})\,, \end{aligned} \tag{2}$$

where $Q_{\mathbf{S}^n}(\vec{\mathbf{x}})$ is the location vector of an optimal exploration focal point in $\mathbf{S}^n$ nearest to $\vec{\mathbf{x}}$, and $s^2(O_{\mathbf{S}^n})$ is the variance of the posterior odds.

RESULTS: ESTIMATION OF THE NUMBER OF EXPLORATION FOCAL POINTS

Assume

- $r = 9$ based on the nine predicted out of 14 undiscovered epithermal occurrences in training set 1
- $p = 0.0025$ based on the average posterior probabilities of prospective pixels in the input WofE prospectivity model

With these assumptions we derive $n = 6280$.
Instead of $p = 0.0025$, we used $p = 0.6$ based on the approximate prediction rate of the input WofE model.
Accordingly, $n = 22$

RESULTS (cont. . .): OPTIMIZED TARGET ZONES

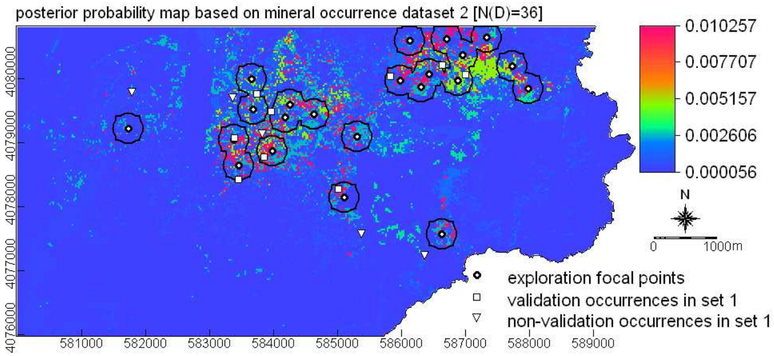

Figure: Optimal exploration target zones defined by buffering to 238 m each of the optimal exploration focal points.

RESULTS (cont. . .): OPTIMIZED TARGET ZONES

- Total area represented by the 6280 unit cells is approximately $6280 \times 25^2 = 3925000\,\mathrm{m}^2$.
- Delineated sub-area of $3925000/22 = 178409\,\mathrm{m}^2$
- If assumed undiscovered deposit is within a radius of $\sqrt{178409/\pi} = 238\,\mathrm{m}$ $(\text{area of circle} = \pi \times \text{radius}^2)$ around a derived optimal exploration focal point – then close.
- Each of the 22 allocated focal points of exploration targets was thus buffered to a radius of 238 m to delineate exploration zones.

RESULTS (cont. . .): OPTIMIZED TARGET ZONES

- Seven of the nine (assumed) undiscovered occurrences, delineated by the WofE model out of the 14 cross-validation undiscovered occurrences, are within the 238 m buffered exploration target zones.
- The result of this analysis indicates that allocated focal points of exploration targets are proximal to undiscovered epithermal occurrences.

Outline

1. Introduction to Remote Sensing
2. Optimized sampling schemes case studies
   - Deriving optimal exploration target zones
   - Optimum sampling scheme for surface geochemical characterization of mine tailings

BACKGROUND AND OBJECTIVE OF STUDY

- Mine wastes contain concentrations of metals.
- Metals – leached from mine wastes – contaminating nearby ecosystems.
- Geochemical characterization of mine waste – useful in decision making – to protect the surrounding environment.
- Such geochemical characterization would entail surface (to subsurface) sampling, which could be labor or cost intensive.

BACKGROUND AND OBJECTIVE OF STUDY (cont. . .)

- Metals in mine waste – hosted by acid-generating sulphide-rich minerals.
- Such minerals are difficult to detect or identify by using current remote sensing techniques using multispectral or even hyperspectral data.
- Certain sulphide-rich minerals weathers to a series of secondary iron-bearing sulfates/hydroxides/oxides and have diagnostic spectral features, which enable their detection or identification with analytical techniques using remote sensing.
- Remote sensing technology potentially provides an indirect tool for surface characterization of mine waste impoundments with oxidizing sulphide-rich materials.

BACKGROUND AND OBJECTIVE OF STUDY (cont. . .)

- Given a model of spatial distribution of secondary iron-bearing oxides/hydroxides, the problem is how to design a sampling scheme that would adequately capture spatial distribution of certain groups of metals.
- The case study presented in this research attempts to model spatial relationships between a multi-element signature and abundance estimates of secondary iron-bearing minerals in mine tailings dumps.

STUDY SITE

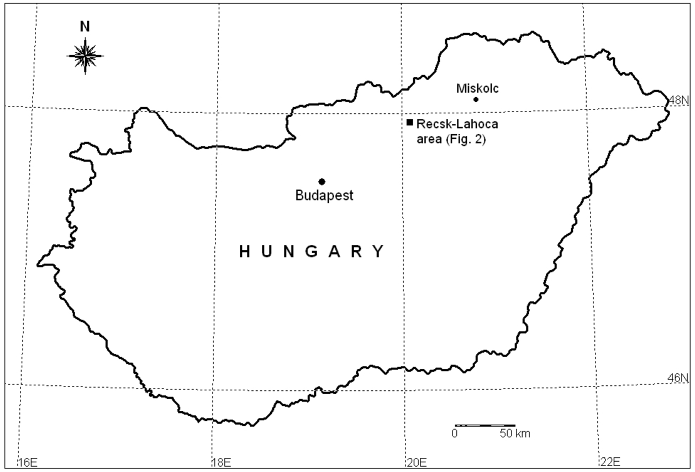

Figure: Study area: Recsk: Hungary.

STUDY SITE (cont. . .)

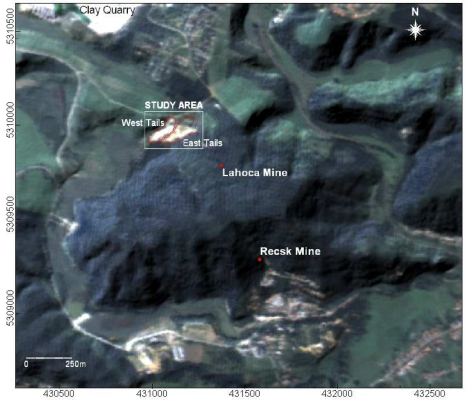

Figure: The Recsk-Lahóca area shown in pseudo-natural color composite image using DAIS data (red = ch10, green = ch5, blue = ch1) fused with a digital elevation model. Map coordinates are in meters (UTM projection, zone 34N).

STUDY SITE (cont. . .)

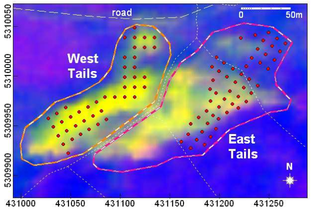

Figure: The “East Tails” and the “West Tails” shown in a color composite image of the DAIS data. Image of ratios of ch17 to ch28 (representing ferrihydrite reflectance and absorption peaks, respectively) was used as red band. Image of ratios of ch13 to ch25 (representing jarosite reflectance and absorption peaks, respectively) was used as green band. Image of ratios ch32 to ch1 (representing non-iron-bearing minerals) was used as blue band. Red dots are locations of mine tailings samples. Short dashed lines in the image represent drainage lines occupied by either active or non-active streams during the field sampling campaign.

DATA USED – HYPERSPECTRAL

- Study site – Recsk – Hungary.
- Digital Imaging Spectrometer – DAIS-7915 – 79 channel hyperspectral image.
- Spectral range from visible (0.4 μm) to thermal infrared (12.3 μm).
- Spatial resolution 3–20 m depending on the carrier aircraft altitude.
- The first 32 channels, spectral range 406–1035 nm, where iron-bearing oxides/hydroxides/sulphates have diagnostic features were found useful for this study.

DATA USED – MINE TAILINGS

- Samples from the tailings – 53 samples were collected in the East Tails and 44 in the West tails.
- Samples of tailings were collected at 10m×10m grid points in portions of the tailings dumps with almost no vegetation cover within 3 m radius.
- Concentrations of As, Cd, Cu, Fe, Mn, Ni, Pb, Sb and Zn in the decomposed samples were determined using the ICP-AES analyzer.

DATA USED – MINE TAILINGS (cont. . .)

Table: Elementary statistics of original geochemical data and skewness of $\log_e$-transformed data. All concentrations are in ppm except where stated.

	East Tails samples ($n = 53$):					
Element	Min	Max	Mean	Std. Dev.	Skewness	Skewness ($\log_e$)
As	48.6	1568.0	266.3	273.9	2.74	0.67
Cd (ppb)	190.0	540.0	323.2	78.2	0.27	−0.28
Cu	85.5	1483.7	354.8	303.3	2.22	0.91
Fe (%)	1.5	3.7	2.8	0.4	-0.49	−1.11
Mn	17.7	766.4	128.4	140.2	3.17	0.41
Ni (ppb)	100.0	4340.0	1129.2	903.5	2.16	−0.36
Pb	14.0	251.8	50.9	52.1	2.27	0.92
Sb (ppb)	5.0	160.0	36.9	31.2	1.59	−0.17
Zn	42.6	762.8	124.4	111.8	3.96	1.14

DATA USED – MINE TAILINGS (cont. . .)

Table: Elementary statistics of original geochemical data and skewness of $\log_e$-transformed data. All concentrations are in ppm except where stated.

West Tails samples ($n = 44$):						
Element	Min	Max	Mean	Std. Dev.	Skewness	Skewness ($\log_e$)
As	196.3	2789.3	625.9	452.0	3.05	0.73
Cd (ppb)	140.0	720.0	275.7	121.8	2.42	1.19
Cu	303.0	2064.7	889.9	476.2	1.12	0.09
Fe (%)	1.4	3.2	2.3	0.4	0.40	−0.06
Mn	15.1	207.6	52.6	34.8	2.40	0.33
Ni (ppb)	60.0	1370.0	371.1	285.6	2.07	−0.06
Pb	40.4	806.9	192.0	169.8	2.24	0.47
Sb (ppb)	5.0	420.0	84.4	76.9	2.75	−0.31
Zn	68.7	776.7	275.2	179.6	1.18	0.06

DATA USED – MINE TAILINGS (cont. . .)

Table: Correlation coefficients for the tailings geochemical data. ^{a} denotes values are significant at $\alpha = 0.05$.

East Tails samples ($n = 53$):

	As	Cd	Cu	Fe	Mn	Ni	Pb	Sb	Zn
As	1.000								
Cd	0.106	1.000							
Cu	0.452^a	−0.358^a	1.000						
Fe	0.118	0.904^a	−0.457^a	1.000					
Mn	−0.412^a	0.373^a	−0.096	0.228	1.000				
Ni	−0.485^a	0.591^a	−0.228	0.464^a	0.835^a	1.000			
Pb	0.475^a	−0.513^a	0.576^a	−0.509^a	−0.458^a	−0.596^a	1.000		
Sb	0.429^a	−0.128	0.440^a	−0.191	−0.186	−0.333^a	0.490^a	1.000	
Zn	0.152	−0.373^a	0.596^a	−0.513^a	−0.027	−0.130	0.727^a	0.359^a	1.000

DATA USED – MINE TAILINGS (cont. . .)

Table: Correlation coefficients for the tailings geochemical data. ^{a} denotes values are significant at $\alpha = 0.05$.

West Tails samples ($n = 44$):									
	As	Cd	Cu	Fe	Mn	Ni	Pb	Sb	Zn
As	1.000								
Cd	0.446^a	1.000							
Cu	0.812^a	0.339^a	1.000						
Fe	0.253	0.423^a	−0.013	1.000					
Mn	−0.101	0.412^a	−0.096	0.403^a	1.000				
Ni	−0.300^a	0.279	−0.289	0.418^a	0.902^a	1.000			
Pb	0.626^a	0.315^a	0.481^a	−0.002	−0.075	−0.193	1.000		
Sb	0.623^a	0.445^a	0.655^a	0.287	0.155	0.030	0.506^a	1.000	
Zn	0.550^a	0.432^a	0.610^a	−0.250	−0.113	−0.229	0.645^a	0.464^a	1.000

DATA USED – MINE TAILINGS (cont. . .)

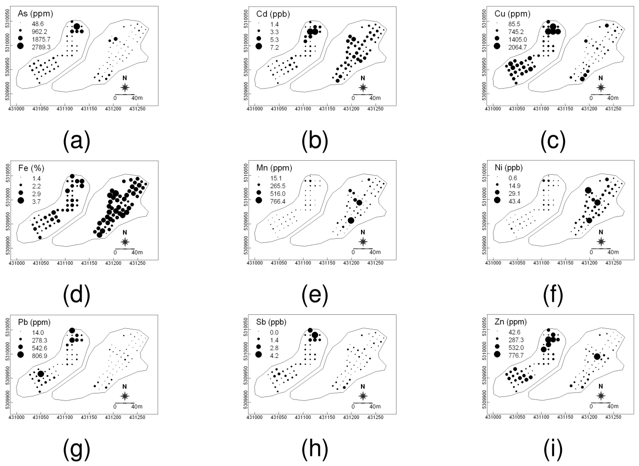

Figure: Element concentrations in samples from the East Tails and the West Tails.